Biochemical Pharmacology 224 (2024) 116252

Contents lists available at ScienceDirect

Biochemical Pharmacology

journal homepage: www.elsevier.com/locate/biochempharm

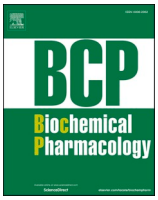

ALDH1A1 confers resistance to RAF/MEK inhibitors in melanoma cells by maintaining stemness phenotype and activating PI3K/AKT signaling

Valerio Ciccone [a], Vittoria Simonis [a], Cinzia Del Gaudio [a], Claudio Cucini [a], Marina Ziche [b], Lucia Morbidelli [a], Sandra Donnini [a,*]

[a] Department of Life Sciences, University of Siena, Siena I-53100, Italy
[b] Department of Medicine, Surgery and Neurosciences, University of Siena, Siena I-53100, Italy

ARTICLE INFO

Keywords:
ALDH1A1
Melanoma
Stemness
Target therapy resistance
RAF/MEK inhibitors resistance

ABSTRACT

The mitogen-activated protein kinase (MAPK/ERK) pathway is pivotal in controlling the proliferation and survival of melanoma cells. Several mutations, including those in BRAF, exhibit an oncogenic effect leading to increased cellular proliferation. As a result, the combination therapy of a MEK inhibitor with a BRAF inhibitor demonstrated higher efficacy and lower toxicity than BRAF inhibitor alone. This combination has become the preferred standard of care for tumors driven by BRAF mutations.

Aldehyde dehydrogenase 1A1 (ALDH1A1) is a known marker of stemness involved in drug resistance in several type of tumors, including melanoma. This study demonstrates that melanoma cells overexpressing ALDH1A1 displayed resistance to vemurafenib and trametinib through the activation of PI3K/AKT signaling instead of MAPK axis. Inhibition of PI3K/AKT signaling partially rescued sensitivity to the drugs. Consistently, pharmacological inhibition of ALDH1A1 activity downregulated the activation of AKT and partially recovered responsiveness to vemurafenib and trametinib. We propose ALDH1A1 as a new potential target for treating melanoma resistant to MAPK/ERK inhibitors.

1. Introduction

Cutaneous melanoma, due to its high heterogeneity and metastatic potential, represents the most lethal form of skin cancer. The incidence of melanoma has been increasing in recent years. The prognosis for this tumor is unfavorable, particularly in advanced and metastatic stages of the disease. The progression and aggressiveness of melanoma are attributable to the high plasticity of tumor cells, thus resulting in potential for dissemination and resistance to drug treatments [1].

Tumors, including melanoma, harbour heterogeneous clones of cancer stem cells (CSCs) that represent key properties for survival and self-renewal. Melanoma CSCs are a group of quiescent self-renewing cell types pre-existing in primary tumors and located within tumor niches that have an enriched functional potential to drive cancer growth, to reconstruct their heterogeneity [2]. CSCs possess the ability to expand into multiple progenitor lineages and are recognized for their inherent resistance to anticancer therapies. CSCs evade anticancer therapies by remaining quiescent, turn off apoptotic pathways, manage reactive oxygen and nitrogen species (ROS, RNS) and reprogram the tumor microenvironment (TME) to their advantage [3,4].

In recent years, the combination therapy with protein kinase inhibitors (PKIs) of BRAF and MEK, such as vemurafenib and trametinib, has improved the management of unresectable and metastatic cutaneous melanoma. Mutations in BRAF are found in over 50% of melanomas, with $BRAF^{V600E}$ substitutions accounting for 90 % of these cases. This and other oncogenic mutations (e.i. $BRAF^{V600D}$) activate the downstream kinase MEK/ERK within the MAPK pathway, promoting tumorigenesis [5]. Targeting this BRAF mutant kinase by protein kinases

Abbreviations: A.D.U, arbitrary density units; AKT, AKT Serine/Threonine Kinase; ALDH1A1, Aldehyde dehydrogenase 1A1; ANOVA, Analysis of variance; ATCC, American type culture collection; BRAF, B-RAF Proto-oncogene, Serine/Threonine Kinase; BRAFi, BRAF inhibitors; BSA, Bovine serum albumin; CSC, Cancer stem cell; DMSO, Dimethylsulfoxide; DUSP, Dual specificity phosphatase; ERK, Extracellular signal-regulated kinases; FBS, Fetal bovine serum; HRP, Horseradish peroxidase; ICI, Immuno-checkpoint Inhibitor; MAPK, Mitogen activated protein kinase; MEKi, MEK inhibitors; MTT, Methyl thiazole tetrazolium; PBS, Phosphate buffered saline; PI3K, Phosphoinositide 3-kinase; PKIs, Protein kinase inhibitors; RA, Retinoic acid; ROS, Reactive Oxygen Species; RNS, Reactive Nitrogen Species; RTK, Receptor tyrosine kinases; SD, Standard deviation; SKCM, Skin cutaneous melanoma; TCGA, The cancer genome atlas; TME, Tumor microenvironment.

* Corresponding author at: Department of Life Sciences, University of Siena, 2 Via Aldo Moro, Siena I-53100, Italy.
E-mail address: sandra.donnini@unisi.it (S. Donnini).

https://doi.org/10.1016/j.bcp.2024.116252
Received 24 November 2023; Received in revised form 16 April 2024; Accepted 30 April 2024
Available online 1 May 2024

inhibitors (BRAFi and MEKi) demonstrates a striking response in melanoma.

Although the inhibitors have ameliorated the survival rates in significant proportion of patients, many patients who receive BRAFi + MEKi therapy have a limited duration of response, and a predictive biomarker for response has not been identified, suggesting that primary and acquired resistance against BRAFi + MEKi therapy remains an important clinical issue and an unmet medical need.

The current National Comprehensive Cancer Network 2021 and European Society of Medical Oncology guidelines (2019) recommend that the preferred first-line treatment for advanced and metastatic BRAF-mutated melanoma should include therapies with immune checkpoint inhibitors (ICIs) rather than combination therapy with BRAFi + MEKi [6]. In patients with advanced melanoma with a BRAF V600 mutation, the first-line combination consisting of the triplet of vemurafenib + cobimetinib + atezolizumab has demonstrated longer duration of antitumor responses and superiority of progression free survival compared with the BRAFi + MEKi doublet, thus receiving recent FDA approval.

Additionally, because stemness is also a mechanism of resistance to ICIs, understanding the molecular mechanisms that support it is an important goal for more effective targeted therapy.

Several resistance mechanisms have been identified, ranging from the activation of various receptor tyrosine kinases (RTKs) to the triggering of alternative signaling pathways such as PI3K/AKT pathway [7]. Many stemness markers have been identified in solid tumors, including aldehyde dehydrogenase 1A1 (ALDH1A1). ALDH1A1 identifies CSCs in multiple cancers, including breast cancer and melanoma, among others [8]. This enzyme belongs to the ALDH superfamily, which is involved in the oxidation of exogenous and endogenous toxic aldehydes to their respective carboxylic acids. Within the ALDH1A family, ALDH1A1 and ALDH1A3 have been shown to be associated with cellular self-protection, differentiation, expansion, tumor progression and therapy resistance [8]. Based on this evidence, we have previously demonstrated the contribution of ALDH1A1 in rewiring the tumor microenvironment, promoting neoplastic progression and angiogenesis in breast cancer and melanoma cells [3,9].

Increased expression and activity of ALDH1A1 are putative markers of resistance to chemotherapeutic agents. Indeed, ALDH1A1 converts cyclophosphamide into 4-hydroperoxycyclophosphamide, which is an inactive excretory byproduct [10]. Moreover, ALDH1A1 enrichment has been detected in head and neck cancer cell lines exhibiting resistance to cisplatin and 5-fluorouracil [11]. More recently, involvement of ALDH1A1 in resistance of other anticancer treatments, including PKIs, has been documented [12,13], but its action is still unknown.

Indeed, apart from attributing drug resistance to its CSC phenotype-related traits, the molecular mechanism whereby ALDH1 itself induces resistance to PKIs remains unknown.

In light of the complexities related to ALDH1A1 influence on cancer drug response, the present study has investigated the link between ALDH1A1 expression in melanoma cells and the intrinsic resistance to PKIs in 2D and 3D in vitro tumor models. Our study demonstrates that ALDH1A1 activity and expression confer intrinsic PKIs resistance in melanoma cells, reprogramming growth and survival signaling from MEK/ERK to PI3K/AKT.

2. Materials and methods

2.1. Data collection and bioinformatics analyses

The Cancer Genome Atlas (TCGA) database stores high-throughput and clinical data of various tumors from many organs. Transcript profiles of 473 melanoma patients belonging to the TGCA-SKMC project (https://portal.gdc.cancer.gov/projects/TCGA-SKCM) were downloaded and filtered depending on ALDH1A1 expression. Each patient case was linked to its clinical history in order to evaluate differences in melanoma prognosis over ALDH1A1 expression. Further, an additional filtering on "site_of_resection_or_biopsy" was applied by retaining only those observations related to skin tissue. Tumor stages were classified in three major groups: Tis-T0, T1-T2, T3-T4.

We highlighted the correlation between ALDH1A1 and the melanoma stage/size (Tis-T0 vs T1-T2 vs T3-T4), patients' vital status (alive vs dead) and expression in primary or metastatic tumor. Statistical comparisons regarding ALDH1A1 gene expression were performed in the R environment (v. 4.3.1) by employing the Kruskal.test R function for multiple group comparison and the pairwise.wilcox.test R function with Bonferroni correction method for pairwise comparisons.

2.2. Chemicals and reagents

The ALDH1A1 inhibitor CM037 was purchased from ChemDiv Inc. (San Diego, CA, USA). CM037 was dissolved in dimethyl sulfoxide (DMSO) (10 mM). Vemurafenib, a potent inhibitor of $BRAF^{V600}$, and trametinib, a highly specific and potent MEK1/2 inhibitor, were from Selleck Chemicals LLC (Houston, TX, USA) and were dissolved in DMSO (vemurafenib at 10 mM and trametinib at 12.6 mM). Phosphoinositide 3-kinase (PI3K) inhibitor LY294002 (dissolved in DMSO at 50 mM), DMSO, CelLytic MT Cell Lysis Reagent, TWEEN 20, Phosphate Buffered Saline (PBS) and lentiviral particles used to achieve a stable knockdown of target signal were provided by Merck KGaA (Darmstadt, Germany). Lentiviral particles used to generate stable ALDH1A1 overexpressed cultures were from OriGene Technologies (Rockville, MD, USA). The kit for fast staining (fast Panoptic) was from PanReac AppliChem ITW Reagents (Darmstadt, Germany).

2.3. Cell lines and culture conditions

Human malignant melanoma A375 and WM-266–4 cells were purchased from American Type Culture Collection (Manassas, VA, USA). Cells were cultured in Dulbecco's Modified Eagle Medium (DMEM) 4500 high glucose (Euroclone SpA, Milan, Italy) supplemented with 10 % fetal bovine serum (FBS; Euroclone SpA, Milan, Italy), 2 mM glutamine, 100 units/ml penicillin and 0.1 mg/ml streptomycin (Merck KGaA, Darmstadt, Germany). Tumor cells were cultured in 10 cm diameter Petri dishes maintained in a humidified atmosphere with 5 % CO_2. Melanoma cells were propagated by splitting 1:8 twice a week. To achieve a stable ALDH1A1 knockdown (ALDH1A1KD), 1.5×10^5 melanoma cells were seeded on 6-multiplates. When 70 % of confluence was reached, the cells were transduced with lentiviral particles (Merck KGaA Darmstadt, Germany) carrying a scrambled (SC; pLKO.1-puro Empty Vector Control Transduction Particles also from Merck KGaA Darmstadt, Germany) or two ALDH1A1 short hairpin (sh)RNA sequences (TRC N 0,000,276,459 and TRC N 0000276397). The sequences express the puromycin-resistant gene (ALDH1A1KD). A MOI (Multiplicity of Infection) of 10 was applied. The cells were incubated at 37 °C and after 36 h selection began by puromycin treatment for 3 days (2 μg/ml) (Thermo Fisher Scientific, Inc. Waltham, Massachusetts, USA). Stable knockdown was validated by western blot. Selected cells were maintained in complete medium with puromycin (1 μg/ml). The sequence of plasmid inserted in clone 1 cells (ShA) was: 5′-CCG GCA CCG ATT T-GA AGA TTC AA T ACT CGA GTA TTG AAT CTT CAA ATC GGT GTT TTTG-3′. The sequence of plasmid inserted in clone 2 cells (ShB) was: 5′-CCG GCT CTA GCT TTG TCA TAG TTA TCT CGA GAT AAC TAT GAC AAA GCT AGA G-TT TTTG-3′. To obtain stable ALDH1A1 overexpressed cultures (ALDH1A1+), 1.5×10^5 melanoma cells were seeded on 6-multiplates. Lentiviral particles containing nucleotide sequences encoding for ALDH1A1 (Origene RC200723 LentiORF particles, ALDH1A1 (Myc-DDK tagged) – Human, Rockville, MD, USA) were used to infect the cells. The empty vector for overexpression was from OriGene Technologies, Inc. (Rockville, MD, USA) (cat. no. PS100001). A MOI of 10 was applied. The cells were incubated at 37 °C and at 36 h post-infection, G418 (400 μg/ml) (Merck KGaA Darmstadt, Germany) was added to cells and selection was

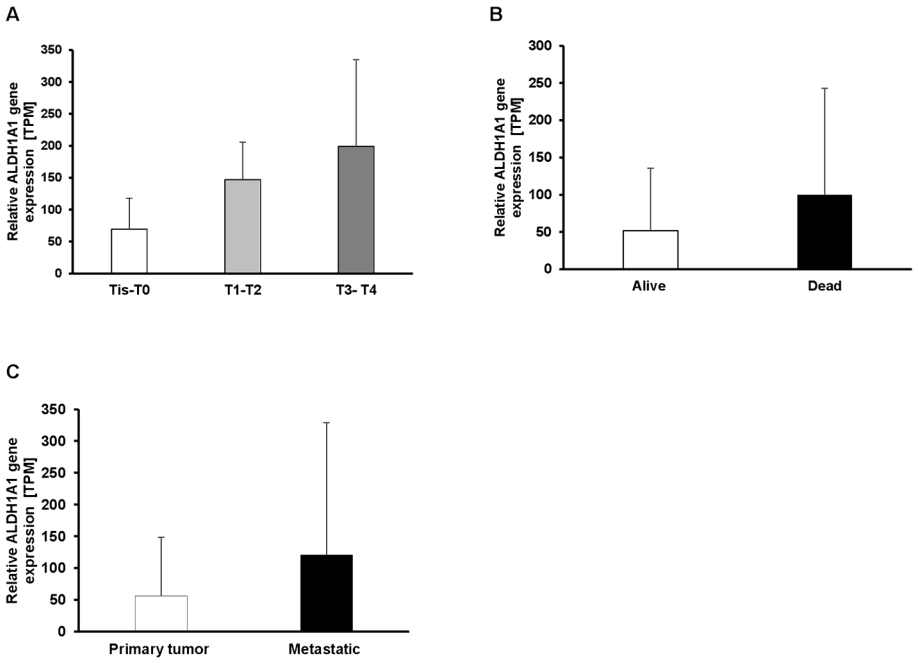

Fig. 1. Increased expression of ALDH1A1 is associated with advanced tumor stage in TCGA-SKCM database. (A). Increased expression of ALDH1A1 was associated with advanced tumor stage in TCGA- SKCM database. (B). Relative ALDH1A1 expression in TCGA-SKCM cases which have different living statuses (alive or dead). (C). Relative ALDH1A1 expression in TCGA-SKCM cases in primary or metastatic tumor. (N = 295).

allowed for 10 days. ALDH1A1 + cells were generated by G418 selection for 10 days. Stable ALDH1A1 overexpression was validated by western blot. Selected cells were maintained in a complete medium with G418 (400 μg/ml) as reported previously [3]. All melanoma cells were expanded and used until 20 passages.

2.4. MTT assay

Cell survival was quantified by MTT (3-(4,5-dimethylthiazol-2-yl)-2,5-diphenyl tetrazolium bromide, Merck KGaA, Darmstadt, Germany). Melanoma cells (3×10^3) were seeded in 96-multiwell plates in medium with 10 % FBS. The next day the cells were treated with increasing concentrations of vemurafenib (0 μM-10 μM), trametinib (0 μM-10 μM) or LY294002 and then grown in complete medium with 10 % FBS at 37 °C. After 24, 48 and 72 h the medium was removed and MTT was added in cell cultures and incubated for 4 h at 37 °C. DMSO (Merck KGaA Darmstadt, Germany) was used to dissolve the formazan salt. Data are reported as the fold change of absorbance measured at 540 nm/well as reported [14], taking as reference the untreated cells.

2.5. Clonogenic assay

For clonogenic assay, cells were plated in 6-multiwell plates (at a density of 100 cells/well) in a medium containing 10 % FBS, kept in a humidified incubator at 37 °C and 5 % CO_2 for 24 h and then treated. When appropriate, cells were pre-treated for 30 min (at 37 °C) with CM037 (10 μM every 24 h) and then treated with vemurafenib (1 μM) or trametinib (1 μM) in medium with 10 % FBS and kept in a humidified incubator for one week. Where indicated, cells were treated with LY294002 at concentration of 1 μM and 5 μM every 48 h. Colonies (>50 cells) were fixed adding fixing for fast staining (panoptic No.1) for 15 min at room temperature and then stained using eosin for fast staining (Panoptic No. 2) for 15 min at room temperature followed by blue dye for fast staining (Panoptic No; Azur B based; PaneReac AppliChem ITW Reagents, Darmstadt, Germany) for 15 min at room temperature. Data are expressed as number and size of colonies [15].

2.6. In vitro tumorsphere formation

The tumorsphere formation assay is an in vitro surrogate that enables the evaluation of sphere formation from dispersed tumoral cells. Melanoma cells (2×10^5 cells/well in 1.5 ml of medium) were distributed into ultralow attachment 6-well plates as reported [9]. Tumorspheres were grown in DMEM-F12 medium (Lonza group Ltd Basel, Switzerland), supplemented with penicillin/streptomycin, L-glutamine (Merck KGaA Darmstadt, Germany), and 10 % FBS for 4 days. During tumorsphere formation, they were treated with vemurafenib (1 μM) and trametinib (1 μM) given every 48 h, in the presence/absence of CM037 (with CM037 1 μM pre-treatment for 30 min at 37 °C and then readded every 48 h). Where indicated, tumorspheres were also treated with LY294002 at concentration of 1 μM and 5 μM each day. After 4 days, tumorspheres were collected and lysed for protein extraction.

2.7. Western blot

Western blot was performed on cell culture lysates and tumorspheres. Melanoma cells (3×10^5/dish) were seeded in 60 mm Petri plates. After adherence, cells were starved for 18 h and where appropriate, pre-treated for 30 min with CM037 (10 μM) and treated with/without vemurafenib (1 μM) or trametinib (1 μM) in medium with 10 % FBS for 4 or 24 h. At the end, cells were washed 2x with cold Dulbecco's Phosphate Buffered Saline (PBS) (Merck KGaA Darmstadt, Germany) and lysed on ice with CelLytic™ MT Cell Lysis Reagent supplemented with 2 mM Na_3VO_4 and 1x Protease inhibitor cocktail for mammalian cells (Merck KGaA Darmstadt, Germany) as described previously [16]. Tumorspheres after 4-day treatment were collected and centrifuged at 300 g for 2 min at 4 °C and the pellets were lysed on ice as reported above. Cell lysates (derived from cell cultures or tumorspheres) were centrifuged at maximum speed for 20 min at 4 °C and the supernatants were then collected. Bradford assay was used to determine the protein concentration. Proteins (50 μg/sample) were separated by polyacrylamide gel electrophoresis (Bolt 4 to 12 %, Bis-Tris, 1.0 mm, Mini Protein Gel, 10-well, from Thermo Fisher Scientific, Inc.). Proteins were transferred onto a nitrocellulose membrane (iBlot 2 Transfer Stacks,

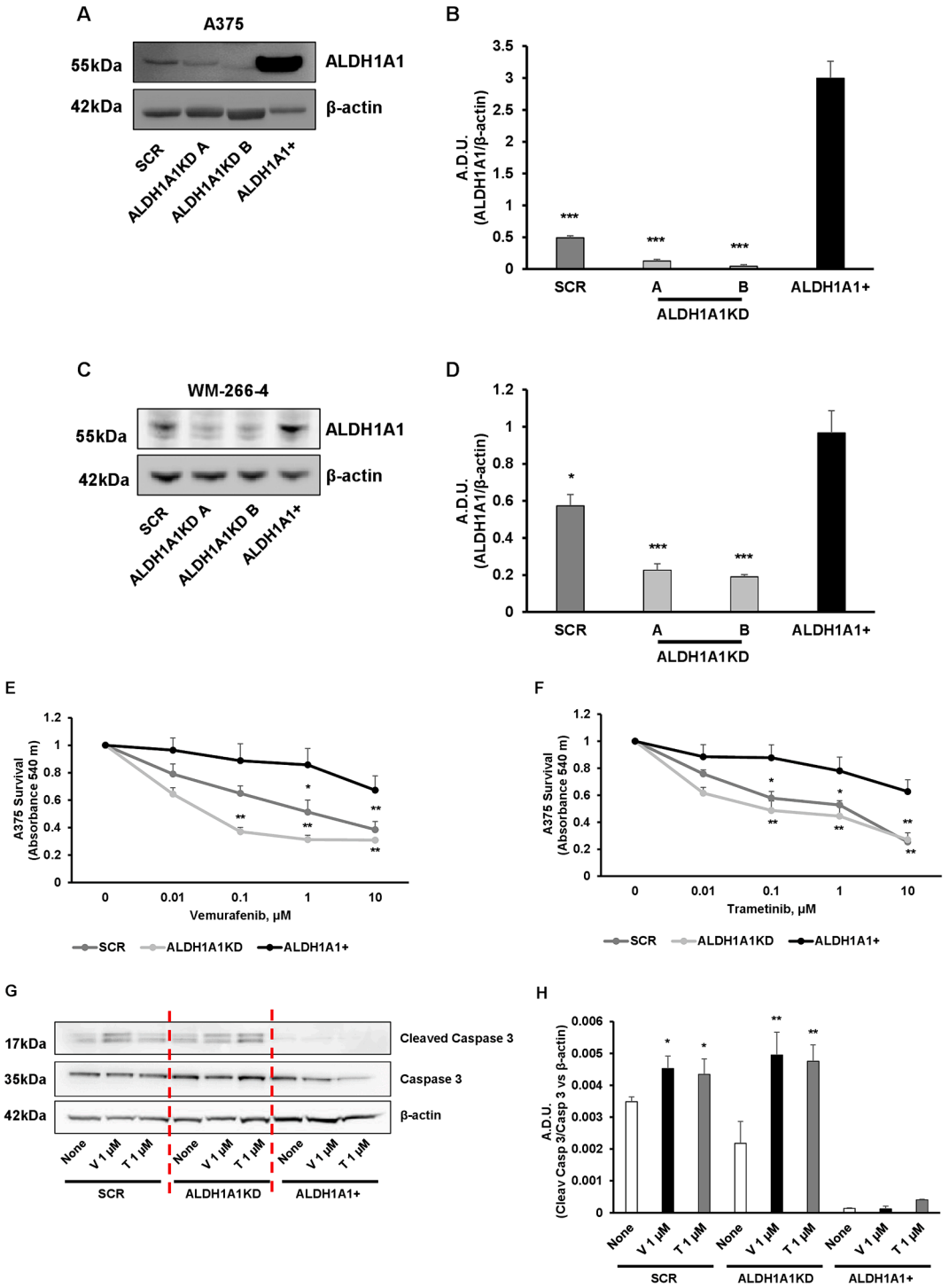

Fig. 2. ALDH1A1 expression in melanoma cells confers resistance to PKIs-reduced survival. Western blot analysis of A375 (A) and WM-266–4 (C) (SCR, ALDH1A1KD clones shA and shB, ALDH1A1+) cultured in 10 % FBS for 48 h. Gel shown is representative of three experiments with similar results. Quantification of ALDH1A1 in A375 (B) and WM-266–4 (D). Arbitrary Densitometry Units (A.D.U.) ± SD were reported as ALDH1A1 vs β-actin (n = 3). * $p < 0.05$ and *** $p < 0.001$ vs. ALDH1A1+ . Survival (MTT test) in A375 treated with increasing concentrations of vemurafenib (E) and trametinib (F) for 48 h (10 % FBS). *$p < 0.05$ and **$p < 0.01$ vs ALDH1A1+ . (G). Caspase 3 cleavage in A375 cells treated with vemurafenib (V) and trametinib (T) (1 μM each) for 4 h. Gel shown is representative of three experiments with similar results. (H). Quantification of blots shown in (G). Arbitrary Densitometry Units (A.D.U.) ± SD were reported as Cleaved-Caspase 3/ Caspase 3 vs β-actin (n = 3). *$p < 0.05$ and **$p < 0.01$ vs untreated cells. Survival of WM-266-4 treated with vemurafenib (I) and trametinib (J) for 48 h (in medium with 10 % FBS). *$p < 0.05$ and **$p < 0.01$ vs ALDH1A1+. (K). Caspase 3 cleavage in WM-266-4 cells treated with trametinib (T) (1 μM) for 4 h. Gel shown is representative of three experiments with similar results. (L). Quantification of blot shown in (K). Arbitrary Densitometry Units (A.D.U.) ± SD were reported as Cleaved-Caspase 3/ Caspase 3 vs β-actin (n=3). *$p < 0.05$ and **$p < 0.01$ vs untreated cells.

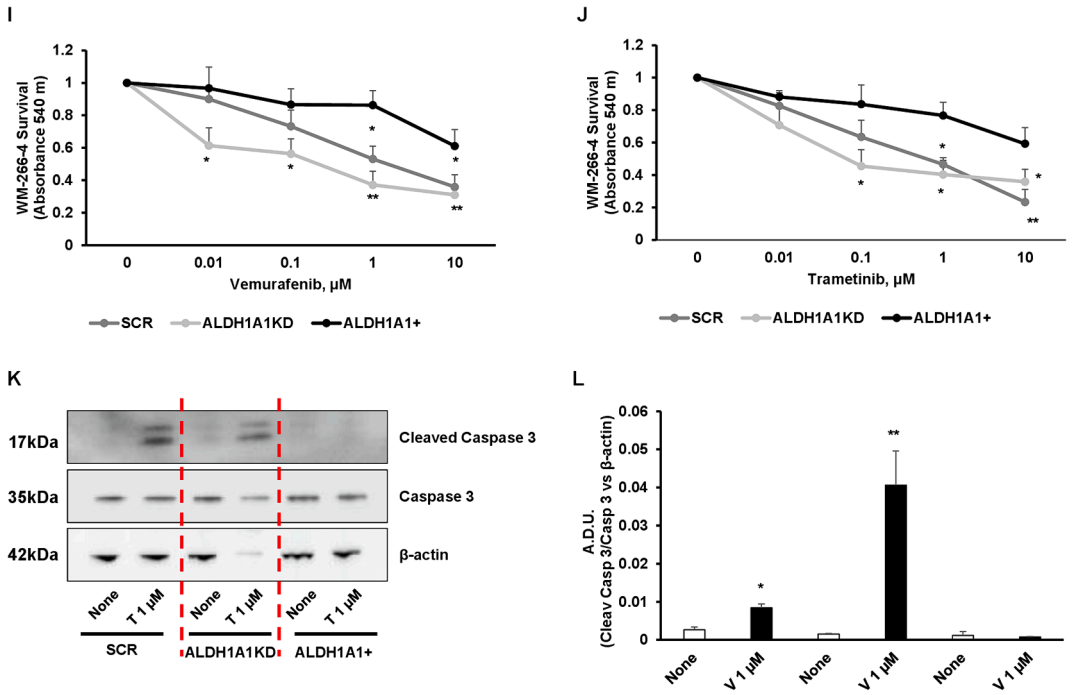

Fig. 2. (*continued*).

nitrocellulose, regular size from Thermo Fisher Scientific, Inc.). Next, membranes were blocked with 5 % non-fat dried milk for 1 h at room temperature, and then incubated at 4 °C overnight with primary antibody including anti-ALDH1A1 (rabbit, 1:1000, cat. n.54135), anti-caspase 3 (rabbit, 1:1000, cat. n.9662), anti-cleaved caspase-3 (Asp175) (rabbit, 1:1000, n. 9661), anti-pERK1/2 (rabbit 1:2000 cat n.4370S), anti-ERK1/2 (rabbit 1:1000 cat n.9102S), anti-pAKT (ser473) (rabbit 1:1000 cat n. 9271S), anti-AKT (mouse 1:2000 cat n.2920S), anti-BRAF (rabbit 1:1000 cat n.14814), anti-DUSP1 (rabbit 1:1000 cat n.35217S), anti-DUSP6 (rabbit 1:1000 cat n. 39441S), anti-CD133 (rabbit 1:1000 cat. no. 64326), anti-Nanog (rabbit 1:1000 cat. no. 3580) and anti-SOX2 (rabbit 1:1000 cat. no. 3579) antibodies. All antibodies were from Cell Signaling Technology, Inc. (Danvers, Massachusetts, USA). Anti-β-actin antibody (mouse, 1:10,000, cat. no. MABT825) was from Merck KGaA (Darmstadt, Germany). The membranes were washed three times (with PBS and TWEEN20 0.5 %) and then incubated with secondary antibodies, HRP conjugated (anti-rabbit, 1:2500, cat. n. W401B; anti-mouse 1:2500, cat. n. W402B, both from Promega Corporation Madison, Wisconsin, USA) at room temperature for 1 h. At the end of incubation, membranes were washed with PBS and TWEEN20 0.5 % (Merck KGaA. (Darmstadt, Germany) three times. The analysis of protein bands was conducted using ChemiDoc XRS (Bio-Rad Laboratories, Inc. Milan, Italy) after incubating at room temperature for 2 min with an enhanced chemiluminescent substrate (Bio-Rad Laboratories, Inc. Milan, Italy) [14]. Each experiment was performed at least three times. Densitometry analysis of immunoblots was performed using Fiji software (64-bit Java 1.8.0_172). The results, presented as arbitrary density units (A.D.U.) ± SD, were normalized against total protein and subsequently β-actin.

2.8. Statistical analysis

The results presented are either indicative or the mean of a minimum of three separate experiments, each conducted in triplicate. Statistical analysis was performed using one-way ANOVA test followed by the Bonferroni test and the unpaired Student *t*-test when appropriate (GraphPad Prism 7; GraphPad Software, Inc.). $P < 0.05$ was considered to indicate a statistically significant difference.

3. Results

3.1. In melanoma cases ALDH1A1 gene is upregulated in a stage-dependent manner and is associated to worst prognosis

Tumor progression and chemotherapy resistance were usually caused by melanoma CSCs [17,18]. In order to understand the impact of ALDH1A1 in melanoma, we investigated the expression profile of 295 TCGA melanoma cases.

Firstly, we found that ALDH1A1 gene expression was upregulated in a stage-dependent manner (Fig. 1A). The clinical data of the T stage was closely correlated with ALDH1A1 expression, the advanced stage was along with the higher expression of ALDH1A1. An increase was observed in T1-T2 and T3-T4 stage compared with Tis-T0 (Fig. 1A). Furthermore, patients with higher ALDH1A1 expression tend to have a worse prognosis, evaluated as vital status (alive or dead) (Fig. 1B) and development of metastasis (Fig. 1C).

This result relates melanoma progression with the gene expression of ALDH1A1.

3.2. ALDH1A1 overexpression confers intrinsic resistance to PKIs-induced apoptosis in melanoma cells

Intrinsic ALDH1A1 serves an important role in stemness, progression and drug response in several solid tumors [8,19]. In order to investigate the role of ALDH1A1 pathway in intrinsic resistance to PKIs in melanoma cells, first we used a loss- and gain-of function strategy. The present study employed the following cell lines: A375 mutated BRAF (V600E) and WM-266–4 metastatic mutated BRAF(V600D) melanoma cells. We created cellular models knocked down for ALDH1A1 (ALDH1A1KD) in A375 and WM-266–4 cells. Melanoma ALDH1A1KD were obtained by using two different shRNA (A and B). For gain-of function model, A375 ALDH1A1+ and WM-266–4 ALDH1A1+ cells were generated (Fig. 2A-D). Melanoma cells transduced with a scrambled sequence were labeled as SCR cells and used as control.

To find out if ALDH1A1 influenced melanoma response to PKIs, a cytotoxicity test (MTT test) on cells grown in monolayer was performed. Under growth-promoting condition of medium with 10 % serum, after

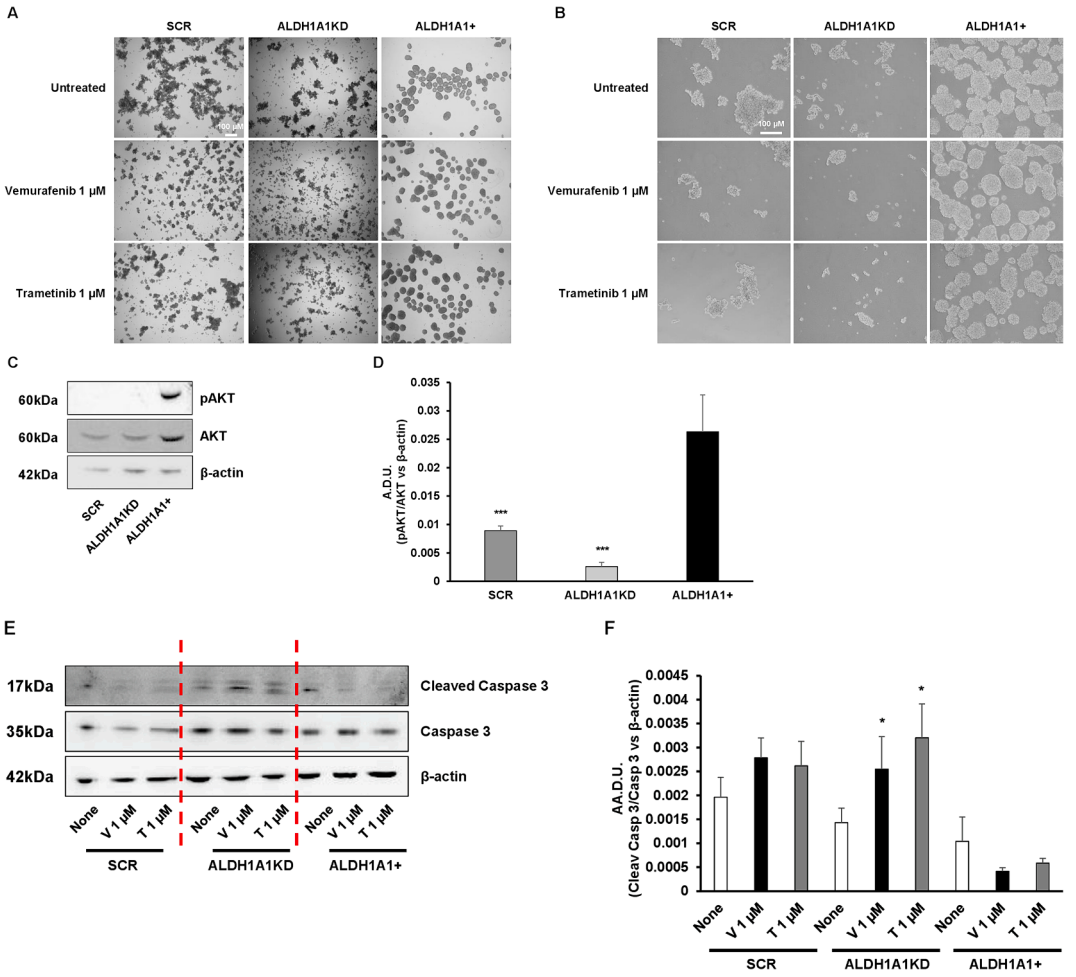

Fig. 3. ALDH1A1 confers resistance to PKIs in stem-like melanoma cells. (A-B). Tumorspheres formation assays in A375 untreated or treated with vemurafenib and trametinib (1 μM each) for 4 days. Scale bar = 100 μm. Tumorspheres photographed at 4x (A) and 10x (B). (C). Western blot analysis of AKT activation (pAKT) in A375 tumorspheres after 4 days of culture. Gel shown is representative of three experiments with similar results. (D). Quantification of blots in C. Arbitrary Densitometry Units (A.D.U.) ± SD were reported as pAKT/AKT vs β-actin. (n = 3). ***p < 0.001 vs ALDH1A1+ . (E). Caspase 3 cleavage in A375 tumorspheres treated with vemurafenib (V) and trametinib (T) (1 μM each) for 4 h. β-actin was used as loading control. Gel shown is representative of three experiments with similar results. (F). Quantification of blots in (E). Arbitrary Densitometry Units (A.D.U.) ± SD were reported as Cleaved-Caspase 3/ Caspase 3 vs β-actin (n = 3). *p < 0.05 vs untreated cells. (G) Tumorspheres formation assays in WM-266–4 untreated or treated with vemurafenib and trametinib (1 μM each) for 4 days. Scale bar = 100 μm. Tumorspheres photographed at 4x (G) and 10x (H). (I). Caspase 3 cleavage in WM-266–4 tumorspheres treated with vemurafenib (V) and trametinib (T) (1 μM each) for 4 h. β-actin was used as loading control. Gel shown is representative of three experiments with similar results. (J). Quantification of blots in (I). Arbitrary Densitometry Units (A.D.U.) ± SD were reported as Cleaved-Caspase 3/Caspase 3 vs β-actin (n = 3). *p < 0.05 vs untreated cells. (K). Quantification of colony formation in A375 SCR, ALDH1A1KD and ALDH1A1+ after 7 days of culture (medium with 10 % FBS). Data are reported as fold change vs SCR, assigned to 1. The graph is the mean data of three independent experiments. (L). Representative images of A375 SCR, ALDH1A1KD and ALDH1A1+ clones. After 7 days of experiment, cells were fixed, stained, and photographed. (M). Quantification of colony formation of A375 treated with vemurafenib and trametinib for 7 days. ***p < 0.001 vs untreated cells. Data are reported as fold change vs untreated cells, assigned to 1. The graph is the mean of three independent experiments. (N). Representative images of clonogenic assay in A375 treated with vemurafenib (V) and trametinib (T). After 7 days of incubation, cells were fixed, stained, and photographed. (O). Colony formation in WM-266–4 after 7 days of culture (10 % FBS). Data are reported as fold change vs SCR, assigned to 1. The graph is the mean data of three independent experiments. (P). Quantification of colony formation of WM-266–4 treated with vemurafenib and trametinib (1 μM each) for 7 days. ***p < 0.001 vs untreated cells. Data are reported as fold change vs untreated cells, assigned to 1. The graph is the mean data of three independent experiments. (Q). Representative images of clonogenic assay in WM-266–4 treated with vemurafenib (V) and trametinib (T). After 7 days of incubation, cells were fixed, stained, and photographed.

48 h of treatment, A375 ALDH1A1+ showed a lower response to vemurafenib (Fig. 2E) and trametinib (Fig. 2F) starting from 100 nM up to 10 μM, compared with ALDH1A1KD or SCR cells. PKIs are associated with pro-apoptotic response, the preferred outcome of tumor therapy [20]. Based on these results, we used the concentration of 1 μM and we observed that, after 4 h of treatment, vemurafenib and trametinib remarkably promoted cleavage of caspase 3, the ultimate mediator of apoptosis pathway, in A375 SCR and ALDH1A1KD cells, but not in A375 ALDH1A1+ (Fig. 2G-H). Similar results were observed in WM-266–4, as vemurafenib and trametinib were not able to reduce cell survival in ALDH1A1+ cells (Fig. 2I-J) and trametinib failed to enhance caspase 3 activation in these cells (Fig. 2K-L).

From all these data it results that melanoma ALDH1A1+ cells show a reduced response to vemurafenib and trametinib, which leads to impaired activation of apoptosis.

3.3. *ALDH1A1 confers intrinsic resistance to PKIs and maintains stem-like properties in melanoma cells*

ALDH1A1 is considered a stemness marker for many tumors,

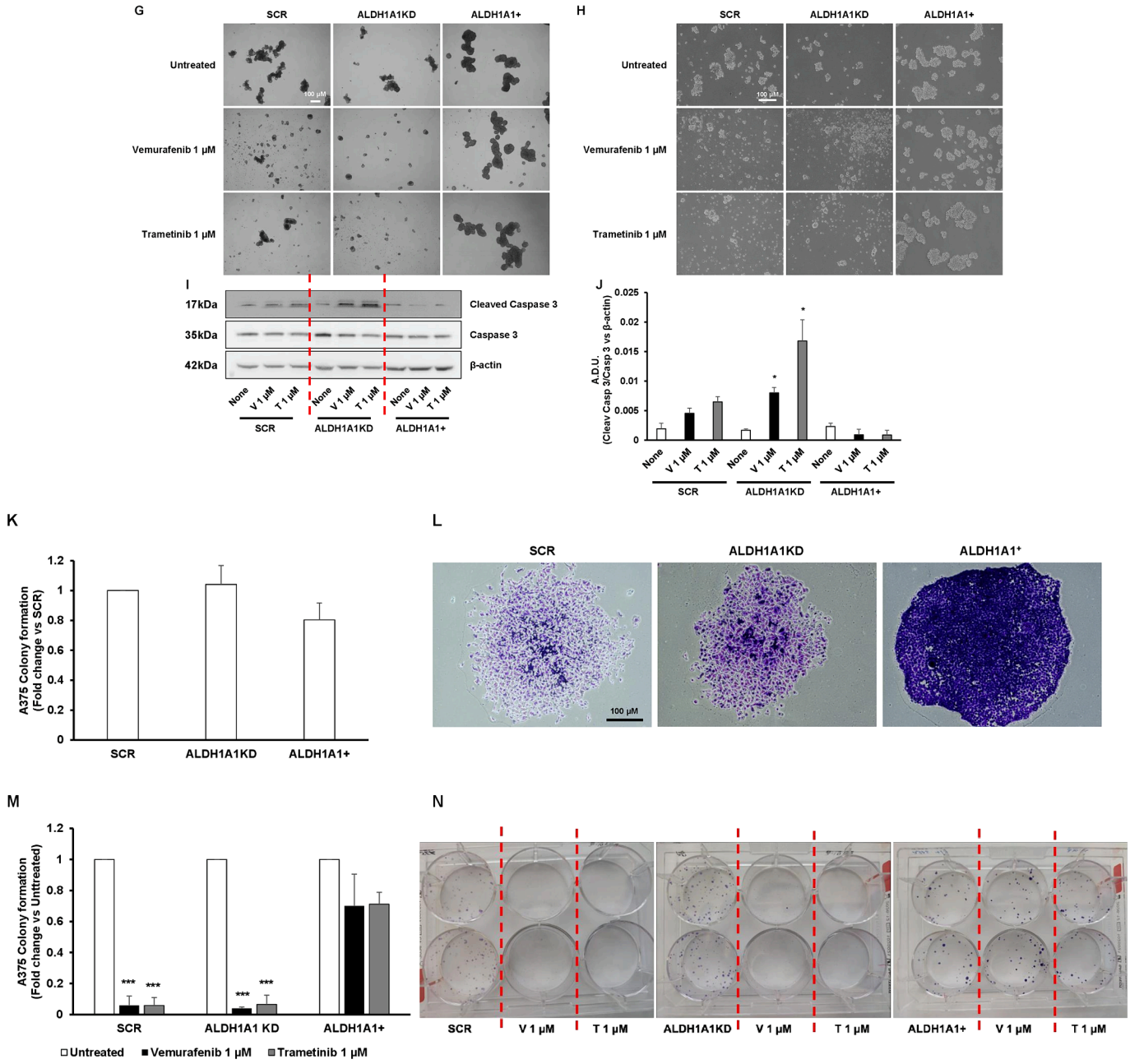

Fig. 3. (*continued*).

including melanoma [8]. To establish the effect of vemurafenib and trametinib on the stemness of melanoma cells, in vitro tumorspheres were set up. In melanoma cells, ALDH1A1KD suppressed the formation of spheroids (Fig. 3A-B for A375 and Fig. 3G-H for WM-266–4, Untreated cells). By contrast, spheres derived from melanoma ALDH1A1+ were denser respect to SCR and ALDH1A1KD, with regular shape and more homogeneous structure (Fig. 3A-B for A375 and Fig. 3G-H for WM-266–4). The dimension and number of melanoma ALDH1A1+ tumorspheres were higher than that of SCR and ALDH1A1KD cells. Molecular analysis revealed a larger activation of pAKT in A375 ALDH1A1+ tumorspheres, in agreement with the maintenance of stemness phenotype (evaluated as tumorspheres formation ability) [21] (Fig. 3C-D). More importantly, high expression of ALDH1A1 enhanced the resistance to PKIs in melanoma tumorspheres, as the number and structure of SCR and ALDH1A1KD melanoma spheres were reduced in presence of vemurafenib and trametinib, while no change was observed for melanoma ALDH1A1+ spheres (Fig. 3A-B for A375 and Fig. 3G-H for WM-266–4). At molecular level, to corroborate the results obtained in monolayer, the analysis of apoptosis marker was performed. A significant activation of caspase 3 was observed in A375 and WM-266–4 ALDH1A1KD tumorspheres after treatment with vemurafenib and trametinib (Fig. 3E-F for A375 and Fig. 3I-J for WM-266–4), while in melanoma ALDH1A1+ cells the expression remains similar to the untreated condition.

ALDH1A1 overexpression also promoted colony formation ability by A375 cells (Fig. 3K). The number of clones was similar among SCR, ALDH1A1KD and ALDH1A1+ cells, but the structure of A375 ALDH1A1+ clones was more compact, aggregated and with regular edges (Fig. 3K-L). Of note, SCR and ALDH1A1KD melanoma cells showed a reduction of clones when treated with vemurafenib and trametinib (Fig. 3M-N for A375 and Fig. 3P-Q for WM-266–4), while melanoma ALDH1A1+ cells continued to exhibit high clonogenicity.

Collectively, these findings suggest that ALDH1A1 mediates stemness phenotype and resistance to PKIs in melanoma cells.

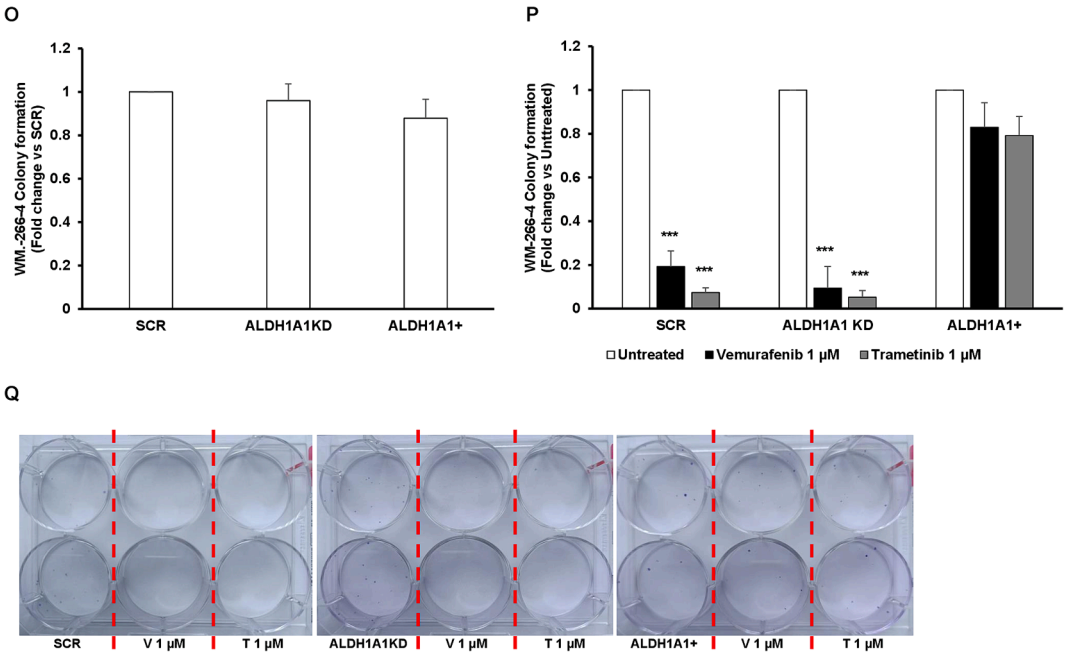

Fig. 3. (*continued*).

3.4. ALDH1A1 mediates PKIs resistance in melanoma cells by PI3K/AKT pathway activation

Recent research suggests that heightened compensatory signaling via the PI3K/AKT axis may play a critical role in driving resistance in the late stages of the RAF/MEK pathway. [22]. To assess the status of KRAS-related signaling pathways and previously reported mechanisms of MEK inhibitor resistance in the RAF/MEK-resistant cells, we performed immunoblot analysis of key downstream effectors. On these bases, we explored the expression and activation of MAPK/ERK and PI3K/AKT signaling in melanoma cells expressing different levels of ALDH1A1.

Western blot analysis revealed that ALDH1A1 expression in A375 cells induced AKT activation and reduced ERK1/2 phosphorylation, indicating the existence of a relation between ALDH1A1 and PI3K/AKT expression (Fig. 4A-B). On the contrary, ERK1/2, the major indicator of active MAPK signaling, was phosphorylated in the control condition (medium with 10 % FBS) in A375 SCR and A375 ALDH1A1KD, suggesting their greater sensitivity to drugs inhibiting this pathway. A375 ALDH1A1+ displayed a substantially reduced phospho-ERK in comparison to their parental counterparts, indicating that these cell lines have bypassed the necessity of the MAPK signaling pathway for their growth.

To determine whether reduced MAPK/ERK signaling and increased PI3K/AKT axis were responsible for the resistance to PKIs observed in melanoma cells with high ALDH1A1 expression, time course experiments were performed in the three cell lines exposed to vemurafenib or trametinib. Western blot showed that in A375 SCR and A375 ALDH1A1KD after 15 min of treatment, trametinib inhibited ERK1/2 activation (Fig. 4C-D). Consistently, vemurafenib after 30 min reduced ERK1/2 activation (Fig. 4E-F). In A375 ALDH1A1+ we detected no activation of ERK1/2, even under basal condition, which explains the ineffectiveness of the drug.

Next, to deeper investigate the regulation of MAPK/ERK signaling pathway, the expression of dual-specificity phosphatase 1 (DUSP1) and 6 (DUSP6) was assessed. In A375 ALDH1A1+ we found a strong downregulation of DUSP6 expression, consistent with its regulation in an ERK signaling activation-dependent manner (Fig. 4G-H) [23]. DUSP1 levels did not change in all the cell lines analyzed (Fig. 4G-H). Similar results were obtained in WM-266–4, in which a high activation of AKT was observed in WM-266–4 ALDH1A1+ in association with vemurafenib and trametinib resistance (Fig. 4I-K). Furthermore, even in WM-266–4 SCR and ALD1A1KD after 30 min of treatment, vemurafenib and trametinib have been shown to be effective in reducing the activation of ERK1/2, an effect not observed in WM-266–4 ALDH1A1+ (Fig. 4L-M).

Next, to prove the dependency of melanoma ALDH1A1+ by PI3K/AKT signaling, a colony formation test was performed in presence of LY294002, a PI3K inhibitor. We found that in A375 ALDH1A1+ cells the treatment with LY294002 (5 μM) significantly reduced their clonogenicity ability, in terms of clone size, but not in number (Fig. 5A-C). A375 ALDH1A1+ clones showed the highest sensitivity to LY294002, suggesting a strict dependance of these cells to PI3K/AKT pathway in cloning phenotype. Further, to demonstrate that the PI3K/AKT pathway regulates the maintenance of stem-like phenotype in melanoma cells, western blot analysis was performed on ALDH1A1 + tumorspheres. As reported in Fig. 5D-E, LY294002 treatment caused a significant reduction of expression of the stemness markers Nanog and SOX2, with a slight effect on CD133 levels.

MTT survival test revealed an overlapping profile of LY294002 sensitivity among A375 SCR, A375 ALDH1A1KD and A375 ALDH1A1+ cells after 24 h (Fig. 6A), 48 h (Fig. 6B) and 72 h (Fig. 6C) of treatment. Finally, to determine whether PI3K/AKT pathways influenced resistance to PKIs, MTT assay was performed in A375 ALDH1A1+ in presence of vemurafenib or trametinib and LY294002. As reported in Fig. 6D, PI3K/AKT inhibition reversed vemurafenib resistance in A375 ALDH1A1+ up to 1 μM. Consistently, a rescue of trametinib sensitivity was also observed in A375 ALDH1A1+ co-treated with LY294002 (Fig. 6E).

Our data suggest the involvement of PI3K/AKT in maintaining melanoma cell stemness, which in turn is responsible for PKIs resistance.

3.5. ALDH1A1 enzymatic activity partially regulates PI3K/AKT activation, and its blocking enhances sensitivity to PKIs

Finally, to explore the contribution of ALDH1A1 enzymatic activity on stable phosphorylation of AKT in ALDH1A1+, a pharmacological approach was used. As reported in Fig. 7A-B, the treatment of ALDH1A1+ cells with CM037, a selective enzyme inhibitor of ALDH1A1, leads to significant decrease of AKT activation. To prove the role of ALDH1A1 metabolic activity on the sensitivity of melanoma cells

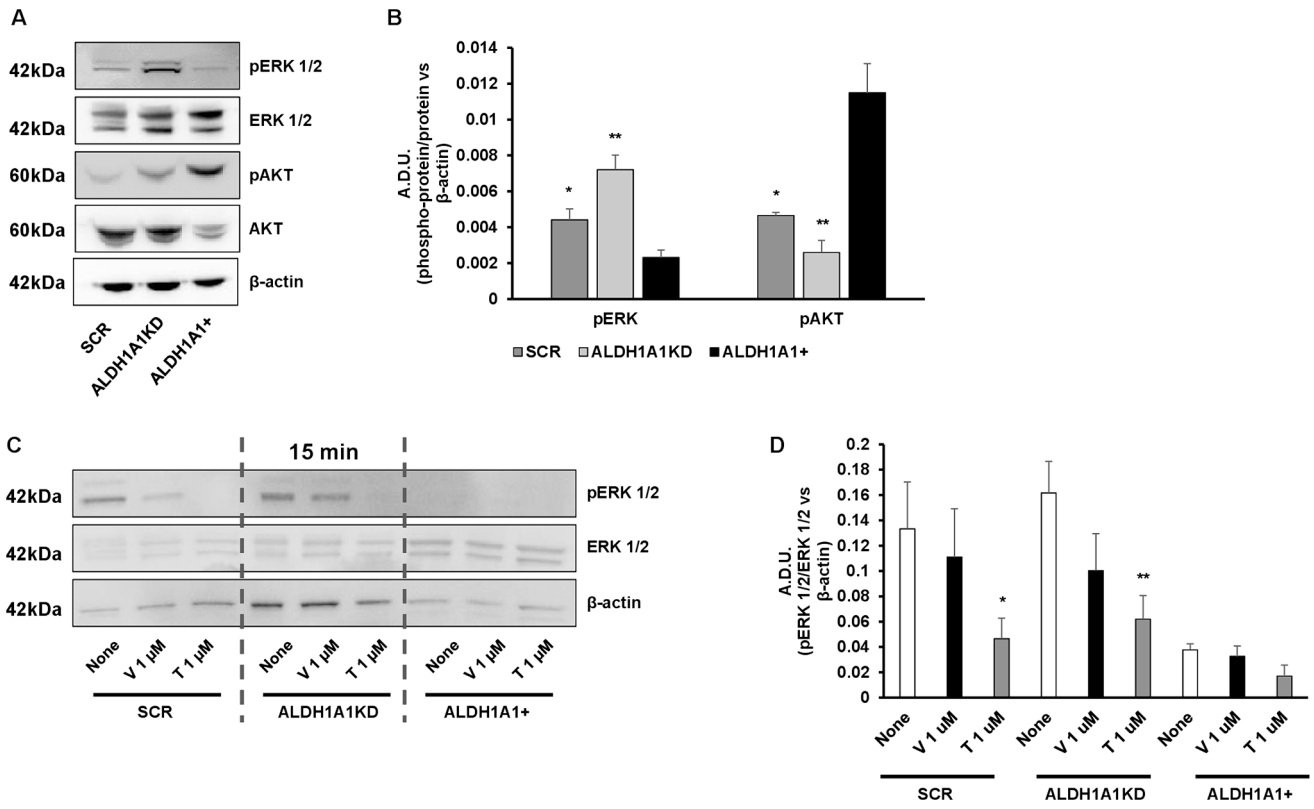

Fig. 4. ALDH1A1 activates PI3K/AKT in melanoma cells. (A). Activation of MAPK/ERK1/2 and PI3K/AKT in A375. Cells were starved for 18 h and then treated with medium with 10 % FBS for 15 min. Gel shown is representative of three experiments with similar results. (B). Quantification of blots in (A). Arbitrary Densitometry Units (A.D.U.) ± SD were reported as phospho-protein/protein vs β-actin (n = 3). *p < 0.05 and **p < 0.01 vs ALDH1A1+ . (C). Mechanism of action of vemurafenib (V) and trametinib (T) in A375 cells after 15 min of treatment. Cells were starved for 18 h and treated with medium with 10 % FBS and PKIs for 15 min. Gel shown is representative of three experiments with similar results. (D). Quantification of blots in (C). Arbitrary Densitometry Units (A.D.U.) ± SD were reported as pERK1/2/ERK1/2 vs β-actin (n = 3). *p < 0.05 and **p < 0.01 vs untreated cells. (E). Mechanism of action of vemurafenib (V) and trametinib (T) in A375 cells after 30 min of treatment. Cells were starved for 18 h and treated with 10 % FBS and PKIs for 30 min. Gel shown is representative of three experiments with similar results. (F). Quantification of blots in (E). Arbitrary Densitometry Units (A.D.U.) ± SD were reported as pERK1/2/ERK1/2 vs β-actin (n = 3). *p < 0.05 vs untreated cells. (G). Western blot analysis in A375 cells treated with 10 % FBS for 24 h. Gel shown is representative of three experiments with similar results. (H). Quantification of blots in (G). Arbitrary Densitometry Units (A.D.U.) ± SD were reported as protein vs β-actin (n = 3). *p < 0.5 and ***p < 0.001 vs ALDH1A1+ . (I). Activation of MAPK/ERK1/2 and PI3K/AKT in WM-266–4. Cells were starved for 18 h and then treated with 10 % FBS for 15 min. β-actin was used as loading control. Blots are representative of three experiments. (J). Quantification of blots in (I). Arbitrary Densitometry Units (A.D.U.) ± SD were reported as phospho-protein/protein vs β-actin (n = 3). *p < 0.05 and ***<0.001 vs untreated cells. (K). Quantification of blots in I for DUSP6. Arbitrary Densitometry Units (A.D.U.) ± SD were reported as DUSP6 vs β-actin (n = 3). **p < 0.01 vs ALDH1A1+ . (L). Mechanism of action of vemurafenib (V) and trametinib (T) in WM-266–4 cells after 30 min of treatment. Cells were starved for 18 h and treated with 10 % FBS and PKIs for 30 min. Gel shown is representative of three experiments with similar results. (M). Quantification of blots in (L). Arbitrary Densitometry Units (A.D.U.) ± SD were reported as pERK 1/2/ERK 1/2 vs β-actin (n = 3). *p < 0.05 vs untreated cells.**

to PKIs, a survival test was performed in presence of CM037.

In both ALDH1A1+, A375 and WM-266–4 cells, the combination of CM037 with vemurafenib or trametinib, as well as with vemurafenib in combination with trametinib, resulted in significant reduced cell survival compared with PKIs alone (Fig. 7C and E), indicating that inhibition of ALDH1A1 enzymatic activity might restore MAPK sensitivity by reducing AKT activation. Further, the clonogenicity ability of melanoma ALDH1A1+ cells was investigated. As shown in Fig. 7D, CM037 combined with vemurafenib or trametinib enhanced the antitumor activity of PKIs compared with vemurafenib and trametinib alone.

Altogether, the data demonstrate that overexpression of tumor-derived ALDH1A1 mediates intrinsic resistance to RAFi/MEKi in melanoma cells by activating PI3K/AKT signaling.

4. Discussion

The present study aimed to assess the contribution of ALDH1A1 in melanoma on intrinsic resistance to RAFi/MEKi, beside its association with tumor progression. We demonstrated that high expression of ALDH1A1 in melanoma cells suppressed ERK1/2 activation and consequently vemurafenib and trametinib activity, while maintaining the stemness phenotype and activating PI3K/AKT signaling, a common mechanism of adaptive resistance to RAF/MEK inhibition [24,25]. Evidence of the specificity of PI3K/AKT signaling in ALDH1A1 + melanoma resistance to vemurafenib and trametinib was further achieved by pharmacological inhibition of this axis with the inhibitor LY294002, which improved sensitivity to the two drugs. The enzymatic activity of ALDH1A1 is responsible for independence from MAPK signaling and dependency on PI3K/AKT signaling, as CM037, the selective ALDH1A1 inhibitor, partially restored sensitivity to PKIs.

ALDH1A1, located in the cytosol, is an enzyme expressed in various solid tumors, contributing to stem-like characteristics, aggressive traits, and resistance to therapy. [3,9,26,27]. Although the significance of ALDH1A1 in CSCs in conferring multidrug resistance to cytotoxic agents as 5-fluorouracil [28] or cyclophosphamide [29] but also to target therapy [30,31] has been described in several reports, a functional role of ALDH1A1 in resistance to vemurafenib and trametinib has not been determined. Indeed, although ALDH1A1 has been identified as one of

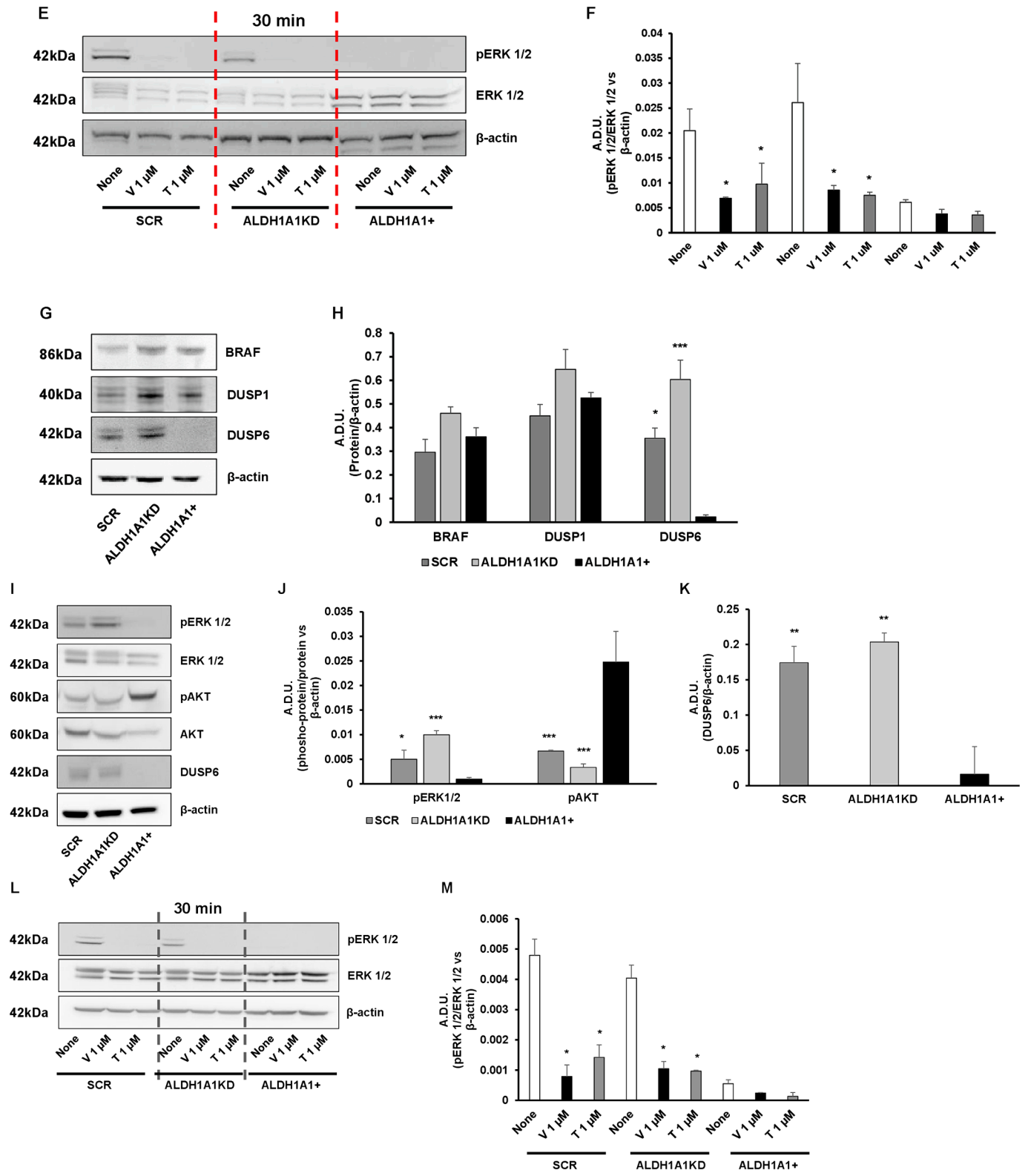

Fig. 4. (*continued*).

the 15 proteins responsible for resistance to MAPK inhibitors in resistant melanoma cells [13], the enzyme function has not been thoroughly investigated. Moreover, while the metabolic activity of ALDH1A1 may explain the detoxification of cyclophosphamide and some other drugs that act through an aldehydic intermediate, and consequently their resistance, the association between ALDH1A1 activity/expression and the mechanism of resistance to other drugs is still poorly known.

Overall, ALDH1A1-mediated drug resistance involves a complex interplay of various mechanisms including detoxification, anti-apoptotic functions, modulation of DNA repair, and alteration of nucleotide metabolism. Undoubtedly, sustaining the status of CSCs capable of inducing cell cycle arrest (quiescent state) might bolster CSCs' resistance

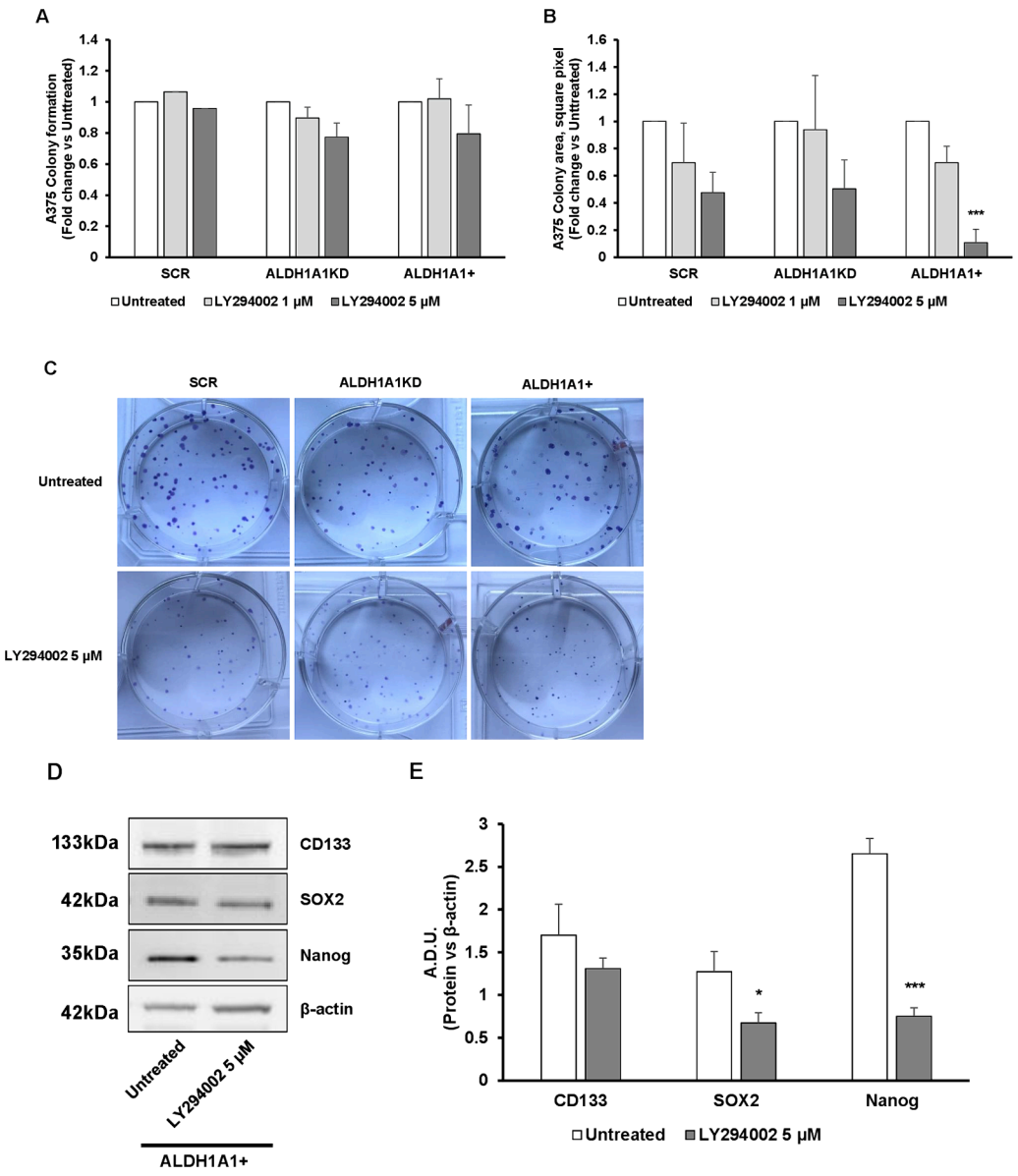

Fig. 5. ALDH1A1 confers clonogenicity to melanoma cells and maintains stemness phenotype through PI3K/AKT signaling. Quantification of colony number (A) or dimensions (B) of A375 treated with LY294002 (1 and 5 μM) for 7 days. ***p < 0.001 vs untreated cells. Data are reported as fold change vs untreated cells, assigned to 1. The graph is the summarized data of three independent experiments. (C). Representative images of clonogenic assay in A375. After 7 days of experiment, cells were fixed, stained, and photographed. (D). Western blot analysis of CD133, Nanog and SOX2 on ALDH1A1 + tumorspheres treated with LY294002 (5 μM) after 4 days of culture. Gel shown is representative of three experiments with similar results. (E). Quantification of blots in (D). Arbitrary Densitometry Units (A.D.U.) ± SD were reported as protein vs β-actin (n = 3). *p < 0.05 and ***p < 0.001 vs untreated cells.

to chemotherapy and radiotherapy [32].

In the present study we observed that ALDH1A1 overexpression ensures cell survival in melanoma cells treated with vemurafenib and trametinib by inhibiting apoptosis in 2D and 3D cell culture models. Melanoma cells overexpressing ALDH1A1 showed the highest stem-like properties evaluated as tumorspheres formation and clonal expansion ability, which were not influenced by PKIs. Many signaling pathways such as WNT, TGFβ, PI3K/AKT, EGFR, and JAK/STAT are commonly activated in CSCs of various tumors to regulate their self-renewal and differentiation state. Hence, the activation of these pathways could potentially be crucial in promoting the proliferation of CSCs and consequently contributing to therapy resistance [33,34]. In our paper we found an hyperactivation of PI3K/AKT in tumorspheres derived from ALDH1A1 + melanoma cells, which was observed in the same cells cultured in 2D, suggesting a critical role of this axis in the maintenance of stem-like properties of melanoma and resistance to PKIs [35]. On the contrary, we found a reduction of ERK1/2 phosphorylation, consistent with MAPK axis suppression, corroborated by impairment of DUSP6 expression which is tightly regulated by ERK1/2 signaling [36]. ERK1/2 function as downstream kinases in the BRAF-MAPK signaling pathway, where they phosphorylate nuclear transcription factors governing cell growth and survival. The phosphorylation of ERK1/2 is frequently employed as a marker for the activation of the MAPK signaling cascade [37,38]. Of note, in our study the expression of ALDH1A1 significantly impaired ERK1/2 phosphorylation but did not affect its expression. These observations lead us to assume a non-transcriptional regulation of ERK1/2 by ALDH1A1, although some papers have documented a nuclear accumulation of ALDH1A1 associated with a poor prognosis in colon cancer [39], and more recently, a report showed an interaction of ALDH1A1 with β-catenin in esophageal squamous cell carcinoma upstream of drug resistance [40].

Activation of the PI3K/AKT signaling pathway might contribute to

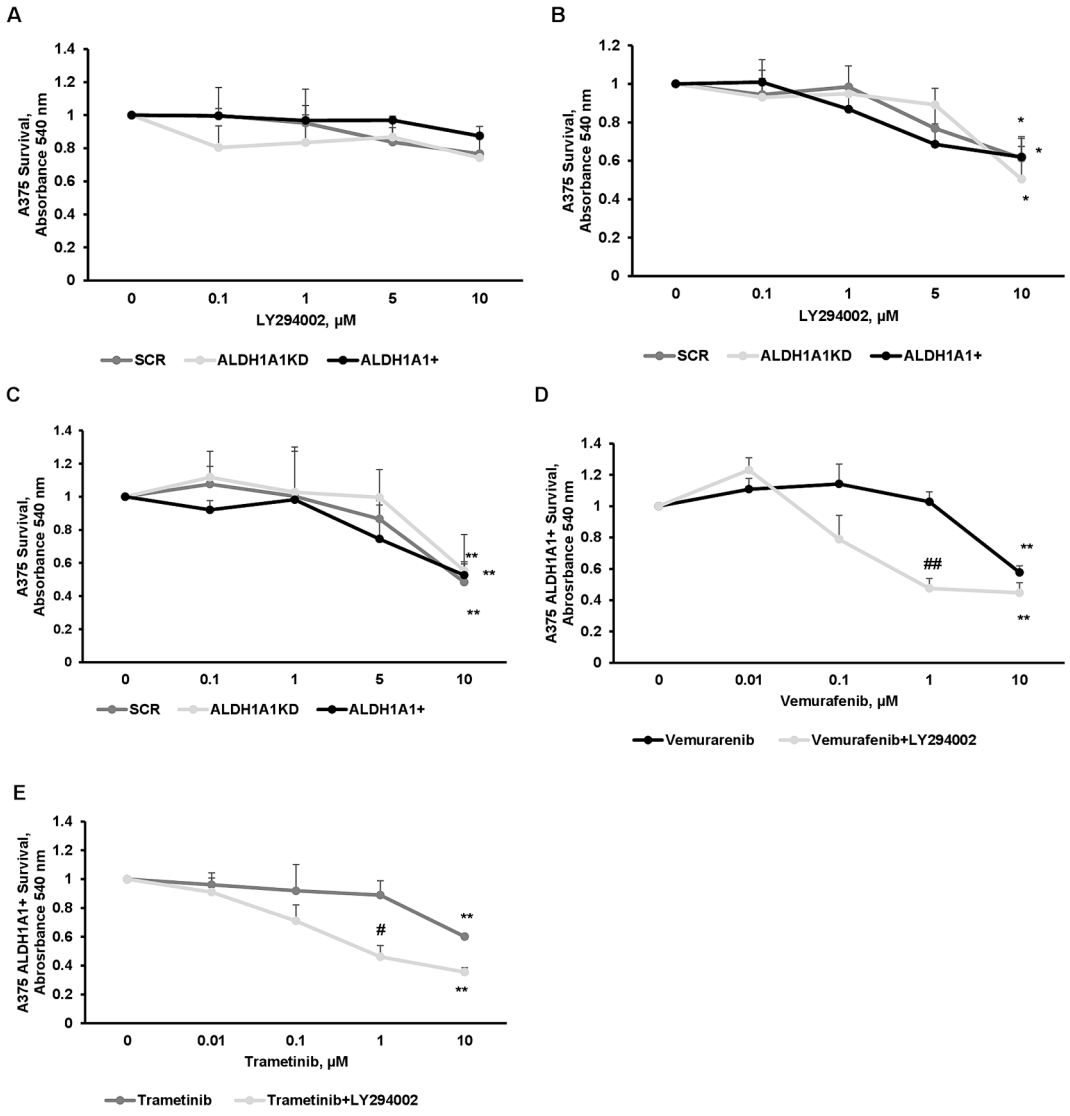

Fig. 6. PI3K/AKT inhibition improves PKIs sensitivity of melanoma cells. Survival in A375 SCR, ALDH1A1KD and ALDH1A1+ treated with increasing concentrations of LY294002 for 24 (A), 48 (B) and 72 h (C) in medium with 10 % FBS. (D). Survival of A375ALDH1A1+ exposed to increasing concentration of vemurafenib and LY294002 (5 μM) for 48 h in 10 % FBS. **p < 0.01 vs untreated cells. ## p < 0.01 vs vemurafenib alone. (E). Survival of A375ALDH1A1+ exposed to increasing concentrations of trametinib and LY294002 (5 μM) for 48 h in medium with 10 % FBS. **p < 0.01 vs untreated cells. # p < 0.05 vs trametinib alone.

the decreased sensitivity to RAFi/MEKi in human melanoma cell lines, as compensatory survival network toward a dedifferentiated phenotype [41]. Indeed, in ALDH1A1 + melanoma cells the treatment with LY294002, a PI3K inhibitor, enhanced vemurafenib and trametinib efficacy in ALDH1A1 + melanoma cells, suggesting that the reduction of the stem-like cell phenotype might improve cell sensitivity to PKIs compared to parental cells. These findings agree with Yoon and co-workers, which showed as PI3K/AKT signaling regulated Nanog to play a critical role in sarcoma CSC maintenance [42].

The molecular mechanism involved in this shift is not completely known, but several hypotheses can be made. Our data show as in ALDH1A1 + melanoma cells pharmacological inhibition of ALDH1A1 (by using CM037) reduces the hyperactivation of AKT, and partially restores responsiveness to vemurafenib and trametinib. As ALDH1A1 mainly converts retinaldehyde to retinoic acid (RA), this finding suggests that RA might contribute to the activation of AKT signaling cascade to protect cells against cell death, with a precedence over the activation of ERK1/2 phosphorylation, as previously reported [43,44]. RA, acting via its nuclear receptors, can also crosstalk with MAPK signaling to stimulate or suppress ERK1/2 phosphorylation, depending on cellular context [45,46]. Further, recent observations showed as RA reduces RAF association with kinase suppressor of Ras1 (Ksr1), the scaffolding protein that facilitates the assembly of the MAPK kinases [47,48]. Further studies are required to assess the role of ALDH1A1-derived RA in resistance to PKIs in melanoma cells.

ALDHs also reduce oxidative damage at cellular and tissue levels by averting the buildup of aldehydes from both endogenous and exogenous sources. ALDHs act as scavenger of ROS because of their ability in metabolizing the aldehydic products generated by the effect of ROS on polyunsaturated fatty acids (PUFAs) present in membrane phospholipids (lipid peroxidation), and inhibition of ALDHs is associated with increased levels of ROS [49]. ROS have been reported to activate the receptors of EGF and PDGF, though without corresponding ligands, which can stimulate MAPK signaling and the subsequent activation of ERK [50]. The hypothetical involvement of ROS scavenging by ALDH1A1 needs however to be deepened in relation to reduced ERK signaling activation and acquired resistance to RAFi/MEKi. A recent study suggests that the stability and subsequent phosphorylation of ERK could potentially be influenced by the levels of tubulin acetylation, a crucial factor in stabilizing microtubules [51]. ALDH1A1-RA signaling

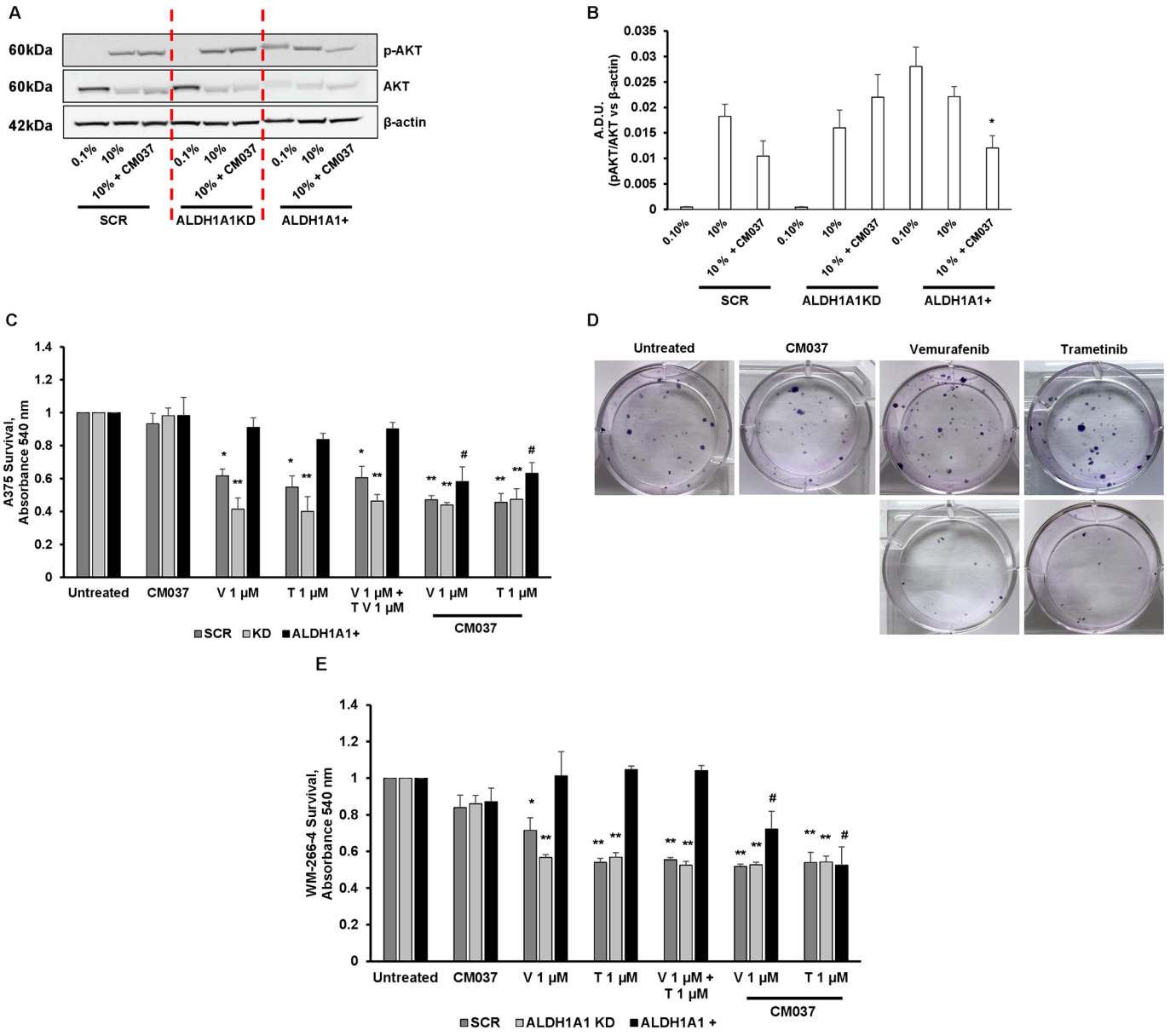

Fig. 7. Pharmacological inhibition of ALDH1A1 activity partially restores responsiveness to vemurafenib and trametinib in A375 cells. (A). Western blot analysis of AKT activation (pAKT) in A375. Cells were starved for 18 h and then treated with CM037 (10 μM for 4 h) and then exposed to 10 % FBS for 15 min. Gel shown is representative of three experiments with similar results. (B). Quantification of blots in (A). Arbitrary Densitometry Units (A.D.U.) ± SD were reported as pAKT/AKT vs β-actin. (n = 3). *p < 0.05 vs 10 % FBS alone. (C). Survival (MTT test) in A375 treated with vemurafenib (V), trametinib (T) or its combination for 48 h (10 μM, 10 % FBS). *p < 0.05 and **p < 0.01 vs untreated cells. # p < 0.05 vs vemurafenib or trametinib alone. (n = 3). (D). Representative images of clonogenic assay in A375 treated every 48 h with CM037 (10 μM, 10 % FBS) and vemurafenib or trametinib (1 μM each). After 7 days of experiment, cells were fixed, stained, and photographed. (E). Survival (MTT test) in WM-266–4 treated with vemurafenib (V), trametinib (T) or its combination for 48 h (10 μM, 10 % FBS). *p < 0.05 and **p < 0.01 vs untreated cells. # p < 0.05 vs vemurafenib or trametinib alone. (n = 3).

could regulate the deposition of both activating and repressive epigenetic marks on histones at target gene promoters.

In conclusion, this work demonstrates that ALDH1A1 overexpression in human melanoma is involved in tumor resistance to RAFi/MEKi by shifting to a stem-like/dedifferentiated phenotype PI3K/AKT-mediated. We conclude that ALDH1A1 may be considered a marker for identifying a subtype of progressive melanoma and a new potential therapeutic target to recover tumor cell sensitivity to PKIs.

Author contributions

SD, MZ, LM and VC conceived the present study. VC, VS, CDG performed methodology, validation, investigation, data analysis. VC wrote the original draft of the manuscript. SD, LM and MZ wrote, reviewed and edited the manuscript. SD supervised and administered the project and acquired funding. All authors reviewed and approved the final manuscript.

CRediT authorship contribution statement

Valerio Ciccone: Writing – review & editing, Writing – original draft, Methodology, Investigation, Data curation, Conceptualization. **Vittoria Simonis:** Methodology, Investigation, Data curation. **Cinzia Del Gaudio:** Methodology, Investigation. **Claudio Cucini:** Methodology, Investigation. **Marina Ziche:** Writing – review & editing, Supervision, Conceptualization. **Lucia Morbidelli:** Writing – review &

editing, Writing – original draft, Supervision, Conceptualization. **Sandra Donnini:** Writing – review & editing, Writing – original draft, Supervision, Project administration, Methodology, Conceptualization.

Declaration of competing interest

The authors declare that they have no known competing financial interests or personal relationships that could have appeared to influence the work reported in this paper.

Data availability

Data will be made available on request.

Acknowledgments

Fondazione Umberto Veronesi, Milan, Italy (Post-doctoral Fellowship 2023 to Valerio Ciccone).

References

[1] S. Diazzi, S. Tartare-Deckert, M. Deckert, The mechanical phenotypic plasticity of melanoma cell: an emerging driver of therapy cross-resistance, Oncogenesis. 12 (1) (2023 Feb 11) 1–7.
[2] M. Najafi, B. Farhood, K. Mortezaee, Cancer stem cells (CSCs) in cancer progression and therapy, J. Cell. Physiol. 234 (6) (2019) 8381–8395.
[3] V. Ciccone, E. Terzuoli, E. Ristori, A. Filippelli, M. Ziche, L. Morbidelli, et al., ALDH1A1 overexpression in melanoma cells promotes tumor angiogenesis by activating the IL-8/Notch signaling cascade, Int. J. Mol. Med. 50 (1) (2022 Jul) 99.
[4] Y. Li, Z. Wang, J.A. Ajani, S. Song, Drug resistance and Cancer stem cells, Cell Commun. Signal. 15 (19) (2021 Feb) 19.
[5] P.A. Ascierto, J.M. Kirkwood, J.J. Grob, E. Simeone, A.M. Grimaldi, M. Maio, et al., The role of BRAF V600 mutation in melanoma, J. Transl. Med. 9 (10) (2012 Jul) 85.
[6] O. Michielin, A.C.J. van Akkooi, P.A. Ascierto, R. Dummer, U. Keilholz, ESMO Guidelines Committee. Electronic address: clinicalguidelines@esmo.org. Cutaneous melanoma: ESMO Clinical Practice Guidelines for diagnosis, treatment and follow-up†, Ann. Oncol. 30 (12) (2019 Dec 1) 1884–1901.
[7] E. Kun, Y.T.M. Tsang, C.W. Ng, D.M. Gershenson, K.K. Wong. MEK inhibitor resistance mechanisms and recent developments in combination trials. Cancer Treatment Reviews [Internet]. 2021 Jan 1 [cited 2023 Jul 3];92. Available from: https://www.cancertreatmentreviews.com/article/S0305-7372(20)30175-4/fulltext.
[8] H. Tomita, K. Tanaka, T. Tanaka, A. Hara, Aldehyde dehydrogenase 1A1 in stem cells and cancer, Oncotarget 7 (10) (2016 Mar 8) 11018–11032.
[9] V. Ciccone, E. Terzuoli, S. Donnini, A. Giachetti, L. Morbidelli, M. Ziche, Stemness marker ALDH1A1 promotes tumor angiogenesis via retinoic acid/HIF-1α/VEGF signalling in MCF-7 breast cancer cells, J Exp Clin Cancer Res. 37 (1) (2018 Dec 12) 311.
[10] M.B. Kastan, E. Schlatter, J.E. Russo, O.M. Colvin, C.I. Civin, J. Hilton, Direct demonstration of elevated aldehyde dehydrogenase in human hematopoietic progenitor cells, Blood 75 (10) (1990 May 15) 1947–1950.
[11] S. Kulsum, H.V. Sudheendra, R. Pandian, D.R. Ravindra, G.R.N. Siddappa, et al., Cancer stem cell mediated acquired chemoresistance in head and neck cancer can be abrogated by aldehyde dehydrogenase 1 A1 inhibition, Mol. Carcinog. 56 (2) (2017) 694–711.
[12] H.M. Lei, K.R. Zhang, C.H. Wang, Y. Wang, G.L. Zhuang, L.M. Lu, et al., Aldehyde dehydrogenase 1A1 confers erlotinib resistance via facilitating the reactive oxygen species-reactive carbonyl species metabolic pathway in lung adenocarcinomas, Theranostics. 9 (24) (2019) 7122–7139.
[13] V. Paulitschke, O. Eichhoff, C. Gerner, P. Paulitschke, A. Bileck, T. Mohr, et al., Proteomic identification of a marker signature for MAPKi resistance in melanoma, EMBO J. 38 (15) (2019 Aug 1) e95874.
[14] V. Ciccone, A. Filippelli, C. Bacchella, E. Monzani, L. Morbidelli, The Nitric Oxide Donor [Zn(PipNONO)Cl] Exhibits Antitumor Activity through Inhibition of Epithelial and Endothelial Mesenchymal Transitions, Cancers 14 (17) (2022 Jan) 4240.
[15] V. Ciccone, M. Monti, E. Monzani, L. Casella, L. Morbidelli, The metal-nonoate Ni (SalPipNONO) inhibits in vitro tumor growth, invasiveness and angiogenesis, Oncotarget 9 (17) (2018 Jan 30) 13353–13365.
[16] V. Ciccone, M. Monti, G. Antonini, L. Mattoli, M. Burico, F. Marini, et al., Efficacy of AdipoDren® in Reducing Interleukin-1-Induced Lymphatic Endothelial Hyperpermeability, J. Vasc. Res. 53 (5–6) (2016) 255–268.
[17] M.R. Makena, A. Ranjan, V. Thirumala, A.P. Reddy. Cancer stem cells: Road to therapeutic resistance and strategies to overcome resistance. Biochimica et Biophysica Acta (BBA) - Molecular Basis of Disease. 2020 Apr 1;1866(4):165339.
[18] H.M. Zhou, J.G. Zhang, X. Zhang, Q. Li, Targeting cancer stem cells for reversing therapy resistance: mechanism, signaling, and prospective agents, Sig Transduct. Target Ther. 6 (1) (2021 Feb 15) 1–17.
[19] A.K. Biswas, S. Han, Y. Tai, W. Ma, C. Coker, S.A. Quinn, et al., Targeting S100A9-ALDH1A1-retinoic acid signaling to suppress brain relapse in EGFR-Mutant lung cancer, Cancer Discov. 12 (4) (2022 Apr 1) 1002–1021.
[20] S. Haferkamp, A. Borst, C. Adam, T.M. Becker, S. Motschenbacher, S. Windhövel, et al., Vemurafenib induces senescence features in melanoma cells, J. Invest. Dermatol. 133 (6) (2013 Jun 1) 1601–1609.
[21] M. Karami fath, Ebrahimi, E. Nourbakhsh, A. Zia Hazara, A. Mirzaei, S. Shafieyari, et al., PI3K/Akt/mTOR signaling pathway in cancer stem cells, Pathol. Res. Pract. 1 (237) (2022 Sep) 154010.
[22] Q. Li, Z. Li, T. Luo, H. Shi, Targeting the PI3K/AKT/mTOR and RAF/MEK/ERK pathways for cancer therapy, Mol. Biomed. 21 (3) (2022 Dec) 47.
[23] Y. Kanda, A. Mizuno, T. Takasaki, R. Satoh, K. Hagihara, T. Masuko, et al., Down-regulation of dual-specificity phosphatase 6, a negative regulator of oncogenic ERK signaling, by ACA-28 induces apoptosis in NIH/3T3 cells overexpressing HER2/ErbB2, Genes Cells. 26 (2) (2021 Feb) 109–116.
[24] J. Meng, H. Peng, B. Dai, W. Guo, L. Wang, L. Ji, et al., High level of AKT activity is associated with resistance to MEK inhibitor AZD6244 (ARRY-142886), Cancer Biol. Ther. 8 (21) (2009 Nov) 2073–2080.
[25] K.K. Wong, J.A. Engelman, L.C. Cantley, Targeting the PI3K signaling pathway in cancer, Curr. Opin. Genet. Dev. 20 (1) (2010 Feb) 87.
[26] V. Ciccone, L. Morbidelli, M. Ziche, S. Donnini, How to conjugate the stemness marker ALDH1A1 with tumor angiogenesis, progression, and drug resistance, Cancer Drug Resist. 3 (1) (2020) 26–37.
[27] Y. Wei, Y. Li, Y. Chen, P. Liu, S. Huang, Y. Zhang, et al., ALDH1: A potential therapeutic target for cancer stem cells in solid tumors, Front Oncol. 28 (12) (2022 Oct) 1026278.
[28] H.Q. Duong, K.S. You, S. Oh, S.J. Kwak, Y.S. Seong, Silencing of NRF2 reduces the expression of ALDH1A1 and ALDH3A1 and sensitizes to 5-FU in pancreatic cancer cells, Antioxidants (basel). 6 (3) (2017 Jul 1) 52.
[29] G. Narendra, B. Raju, H. Verma, O. Silakari, Identification of potential genes associated with ALDH1A1 overexpression and cyclophosphamide resistance in chronic myelogenous leukemia using network analysis, Med. Oncol. 38 (10) (2021 Sep 7) 123.
[30] C.P. Huang, M.F. Tsai, T.H. Chang, W.C. Tang, S.Y. Chen, H.H. Lai, et al., ALDH-positive lung cancer stem cells confer resistance to epidermal growth factor receptor tyrosine kinase inhibitors, Cancer Lett. 328 (1) (2013 Jan 1) 144–151.
[31] W. Yao, L. Wang, H. Huang, X. Li, P. Wang, K. Mi, et al., All-trans retinoic acid reduces cancer stem cell-like cell-mediated resistance to gefitinib in NSCLC adenocarcinoma cells, BMC Cancer 20 (1) (2020 Apr 15) 315.
[32] L.T.H. Phi, I.N. Sari, Y.G. Yang, S.H. Lee, N. Jun, K.S. Kim, et al., Cancer Stem Cells (CSCs) in Drug Resistance and their Therapeutic Implications in Cancer Treatment, Stem Cells Int. 28 (2018) (2018 Feb) 5416923.
[33] H. Rezayatmand, M. Razmkhah, I. Razeghian-Jahromi, Drug resistance in cancer therapy: the Pandora's Box of cancer stem cells, Stem Cell Res Ther. 3 (13) (2022 May) 181.
[34] L. Yang, P. Shi, G. Zhao, J. Xu, W. Peng, J. Zhang, et al., Targeting cancer stem cell pathways for cancer therapy, Sig. Transduct. Target Ther. 5 (1) (2020 Feb 7) 1–35.
[35] S.M.E. Jamal, A. Alamodi, R.U. Wahl, Z. Grada, M.A. Shareef, S.Y. Hassan, et al., Melanoma stem cell maintenance and chemo-resistance are mediated by CD133 signal to PI3K-dependent pathways, Oncogene 39 (32) (2020 Aug) 5468–5478.
[36] Y. Ren, Z. Ouyang, Z. Hou, Y. Yan, Z. Zhi, M. Shi et al. CIC Is a Mediator of the ERK1/2-DUSP6 Negative Feedback Loop. iScience. 2020 Nov 20;23(11):101635.
[37] S. Gouravan, L.A. Meza-Zepeda, O. Myklebost, E.W. Stratford, E. Munthe, Preclinical Evaluation of Vemurafenib as Therapy for BRAFV600E Mutated Sarcomas, Int. J. Mol Sci. 19 (4) (2018 Mar 23) 969.
[38] P.T.C. Wan, M.J. Garnett, S.M. Roe, S. Lee, D. Niculescu-Duvaz, V.M. Good, et al., Mechanism of activation of the RAF-ERK signaling pathway by oncogenic mutations of B-RAF, Cell 116 (6) (2004 Mar 19) 855–867.
[39] C. Kahlert, E. Gaitzsch, G. Steinert, C. Mogler, E. Herpel, M. Hoffmeister, et al., Expression analysis of aldehyde dehydrogenase 1A1 (ALDH1A1) in colon and rectal cancer in association with prognosis and response to chemotherapy, Ann. Surg. Oncol. 19 (13) (2012 Dec) 4193–4201.
[40] W. Wang, S. He, R. Zhang, J. Peng, D. Guo, J. Zhang, et al., ALDH1A1 maintains the cancer stem-like cells properties of esophageal squamous cell carcinoma by activating the AKT signal pathway and interacting with β-catenin, Biomed. Pharmacother. 1 (125) (2020 May) 109940.
[41] E. Corrales, E. Levit-Zerdoun, P. Metzger, R. Mertes, A. Lehmann, J. Münch, et al., PI3K/AKT signaling allows for MAPK/ERK pathway independency mediating dedifferentiation-driven treatment resistance in melanoma, Cell Commun. Signal. 24 (20) (2022 Nov) 187.
[42] C. Yoon, J. Lu, B.C. Yi, K.K. Chang, M.C. Simon, S. Ryeom, et al., PI3K/Akt pathway and Nanog maintain cancer stem cells in sarcomas, Oncogenesis. 10 (1) (2021 Jan 19) 12.
[43] B. Cheng, A.A. Martinez, J. Morado, V. Scofield, J.L. Roberts, S.K. Maffi, Retinoic acid protects against proteasome inhibition associated cell death in SH-SY5Y cells via the AKT pathway, Neurochem. Int. 62 (1) (2013 Jan 1) 31–42.
[44] Y. Lee, J.Y. Lee, M.H. Kim, PI3K/Akt pathway regulates retinoic acid-induced Hox gene expression in F9 cells, Dev. Growth Differ. 56 (7) (2014) 518–525.
[45] S.B. Cheepala, W. Yin, Z. Syed, J.N. Gill, A. McMillian, H.E. Kleiner, et al., Identification of the B-Raf/Mek/Erk MAP kinase pathway as a target for all-trans retinoic acid during skin cancer promotion, Mol. Cancer. 11 (8) (2009 May) 27.
[46] M.l. Zhang, Y. Tao, W.-q. Zhou, P.-c. Ma, Y.-p. Cao, C.-d. He, et al., All-trans retinoic acid induces cell-cycle arrest in human cutaneous squamous carcinoma cells by inhibiting the mitogen-activated protein kinase–activated protein 1 pathway, Clin. Exp. Dermatol. 39 (3) (2014 Apr 1) 354–360.

[47] S.W. Park, J. Nhieu, S.D. Persaud, M.C. Miller, Y. Xia, Y.W. Lin, et al., A new regulatory mechanism for Raf kinase activation, retinoic acid-bound Crabp1, Sci Rep. 29 (9) (2019 Jul) 10929.
[48] M. Radić, I. Vlašić, M. Jazvinšćak Jembrek, A. Horvat, A. Tadijan, M. Sabol, et al., Characterization of Vemurafenib-Resistant Melanoma Cell Lines Reveals Novel Hallmarks of Targeted Therapy Resistance, Int J Mol Sci. 23 (17) (2022 Aug 31) 9910.
[49] G. Vassalli, Aldehyde dehydrogenases: not just markers, but functional regulators of stem cells, Stem Cells Int. 13 (2019) (2019 Jan) e3904645.
[50] J. Zhang, X. Wang, V. Vikash, Q. Ye, D. Wu, Y. Liu, et al., ROS and ROS-Mediated cellular signaling, Oxid. Med. Cell Longev. 2016 (2016) 4350965.
[51] O. Wattanathamsan, N. Chantaravisoot, P. Wongkongkathep, S. Kungsukool, P. Chetprayoon, P. Chanvorachote, et al., Inhibition of histone deacetylase 6 destabilizes ERK phosphorylation and suppresses cancer proliferation via modulation of the tubulin acetylation-GRP78 interaction, J. Biomed. Sci. 30 (1) (2023 Jan 13) 4.